

Article

Pt/Re/CeO₂ Based Catalysts for CO-Water–Gas Shift Reaction: from Powders to Structured Catalyst

Vincenzo Palma ¹, Fausto Gallucci ², Pluton Pullumbi ³, Concetta Ruocco ¹,
Eugenio Meloni ¹ and Marco Martino ^{1,*}

¹ Department of Industrial Engineering, University of Salerno, Via Giovanni Paolo II 132, 84084 Fisciano (SA), Italy; vpalma@unisa.it (V.P.); cruocco@unisa.it (C.R.); emeloni@unisa.it (E.M.)

² Inorganic Membranes and Membrane Reactors, Department of Chemical Engineering and Chemistry, Eindhoven University of Technology, 5600 MB Eindhoven, The Netherlands; f.gallucci@tue.nl

³ Air Liquide, Paris Innovation Campus. 1, chemin de la Porte des Loges, 78350 Les Loges en Josas, France; pluton.pullumbi@airliquide.com

* Correspondence: mamartino@unisa.it; Tel.: +39-089-969275

Received: 6 May 2020; Accepted: 18 May 2020; Published: 19 May 2020



Abstract: This work focuses on the development of a Pt/Re/CeO₂-based structured catalyst for a single stage water–gas shift process. In the first part of the work, the activity in water–gas shift reactions was evaluated for three Pt/Re/CeO₂-based powder catalysts, with Pt/Re ratio equal to 1/1, 1/2 ad 2/1 and total loading \approx 1 wt%. The catalysts were prepared by sequential dry impregnation of commercial ceria, with the salts precursors of rhenium and platinum; the activity tests were carried out by feeding a reacting mixture with a variable CO/H₂O ratio, equal to 7/14, 7/20 and 7/24, and the kinetic parameters were determined. The model which better described the experimental results involves the water–gas shift (WGS) reaction and CO as well as CO₂ methanation. The preliminary tests showed that the catalyst with the Pt/Re ratio equal to 2/1 had the best performance, and this was selected for further investigations. In the second part of the work, a structured catalyst, obtained by coating a commercial aluminum alloy foam with the chosen catalytic formulation, was prepared and tested in different reaction conditions. The results demonstrated that a single stage water–gas shift process is achievable, obtaining a hydrogen production rate of 18.7 mmol/min at 685 K, at $\tau = 53$ ms, by feeding a simulated reformat gas mixture (37.61 vol% H₂, 9.31 vol% CO₂, 9.31 vol% CO, 42.19 vol% H₂O, 1.37 vol% CH₄).

Keywords: hydrogen; water–gas shift; process intensification; structured catalysts; kinetics; aluminum alloy foam; ceria; platinum; rhenium

1. Introduction

The water–gas shift (WGS) reaction [1] is an exothermic reaction, whose process is generally performed through two adiabatic stages, at high (HTS) [2] and low temperatures (LTS) [3]. WGS can be considered as the first syngas purification step to obtain high purity hydrogen, and in fact, it allows for the reduction of the CO percentage and increase of the hydrogen yield in the reformat gas stream [4]. The two-stages process configuration allows us to achieve higher conversions at relatively smaller volumes. The reactors suffer limitations, however, due to the heat of the reaction developed during the process, which induces a temperature gradient on the catalytic bed. The low temperature at the inlet of the bed disfavors the kinetics, while the high temperature at the outlet of the bed thermodynamically limits the conversion. In previous work, the intensification of the WGS reaction through the use of highly thermal conductive structured catalysts has been proposed [5], laying the foundations for the realization of a single stage process [6]. In fact, the use of such a structure [7] assures a redistribution

of the heat of the reaction along the catalytic bed, with benefits in terms of CO conversion [8], while minimizing hot-spot occurrence [9]. Moreover, comparative studies have showed that the shape of the selected structure plays a crucial role in determining the performance of a catalyst. In this context, the use of foam structures guarantees an enhanced axial and radial heat dispersion and mass transfer [10]. Concerning the catalytic formulation, the conventionally used catalysts, both in HTS and LTS processes, are not suitable for the single stage process design, since the latter are readily deactivated at high temperatures and are pyrophoric [11], while the former are not active at low temperatures and present waste toxicity problems [12]. A valuable alternative consists in noble metal-based catalysts [13], supported on reducible oxides such as titania or ceria [14], which are highly active in a wide range of temperatures [15,16]. Among the investigated noble metals, platinum has showed the best compromise between catalytic activity, ease of preparation and stability [17]; moreover, it was reported that rhenium doping enhances the activity of platinum-based catalysts for WGS reactions [18]. Some specific studies have been published on the role of rhenium in these catalytic systems [19], however, the mechanisms have not yet been fully clarified [20]; CO chemisorption measurements have highlighted the better platinum dispersion [21] upon rhenium addition, thus achieving the enhancement in the WGS rate and catalyst stability [22]. Transmission electron microscopy (TEM) and X-ray photoelectron spectroscopy (XPS) studies showed the formation of bimetallic surface clusters between rhenium and platinum; in addition, the stabilization of formate species and the acceleration of the H₂ formation rate were attributed to the presence of rhenium [23]. Azzam et al. studied the Pt–Re/TiO₂ catalytic system and speculated that rhenium remains as oxide, providing an additional redox WGS reaction pathway, in which ReOx is reduced by carbon monoxide generating carbon dioxide and oxidized by H₂O to give hydrogen [24]. Del Villar et al. studied a more complex catalytic system (RePt/CeO₂–TiO₂ catalyst) for the WGS reaction under conditions compatible with a membrane reactor [25]. The authors ascribed the enhanced WGS activity and stability to the improvement in the reduction behavior of highly dispersed CeO₂ and ReOx species, as well as to the close contact between Pt and Re species, which could introduce further redox activity sites and prevent the Pt sintering.

In a process intensification view, the deposition of highly active catalytic formulations on proper structured catalysts was shown to be an effective option for minimizing the typical mass and heat transfer issues of packed bed reactors. In this regard, in our previous papers, we demonstrated that the employment of aluminum open cells foams as structured carrier paddles in the direction of HTWGS-LTWGS integration in a single unit. In fact, due to the high thermal conductivity of the selected material, the heat was redistributed along the catalyst from the outlet to the inlet section with a flatter thermal profile and a global increase of CO conversion [5,7,10].

In the first part of this work, a preliminary study on the use of PtRe/CeO₂-based powder catalysts was reported; the activity of three catalysts with a different Pt/Re ratio (Pt/Re ratio equal to 1/1, 1/2 or 2/1) and total loading of 1 wt% was compared in WGS reaction and a kinetic investigation was performed for the three samples. The kinetic parameters were determined based on the results of three dedicated reaction tests carried out at different H₂O/CO ratio (H₂O/CO ratio equal to 24/7, 20/7 or 14/7). In the second part of the work a structured catalyst was prepared by coating an open cell aluminum alloy foam with cerium oxide and loading the resulting structure with the active species in the ratio which gave the best performance in the preliminary study (Pt/Re = 2/1). The structured catalyst performance was evaluated by feeding the reacting mixture, previously used for the powder catalysts, with a H₂O/CO ratio equal to 24/7 in order to evaluate the effect of the scale up from powder to structured catalyst, in terms of activity. Moreover, the as-obtained structured catalyst was also tested under a simulated reformat gas stream as feed, aiming to evaluate the possibility to realize a single stage water–gas shift reactor, which is highly desirable for the realization of a compact fuel processing system.

2. Results and Discussion

2.1. Powder Catalysts

2.1.1. Characterization Results

Powder catalysts were characterized by means of a series of analytical techniques: energy dispersive X-ray fluorescence (ED-XRF) was used to check the effective metals loading and the effective Pt/Re ratio; X-ray diffraction (XRD) was used to evaluate the crystallite size; Raman spectroscopy (Raman) was used to provide the structural features; transmission electron microscopy (TEM) was used to evaluate the particle size and shape; the temperature programmed reduction with hydrogen (H₂-TPR) to evaluate the reducibility of the catalysts.

The ED-XRF results stated an effective metal loading of 0.88 wt%–0.90 wt% for the three powder catalysts and confirmed the expected Pt/Re ratio (Table 1). The specific surface area measurements calculated with the Brunauer–Emmett–Teller (B.E.T.) method showed a small decrease in the surface area compared to that of the alone ceria (Table 1).

Table 1. Powder catalysts characterization.

	Chemical Composition (wt%)			SSA _{B.E.T.} (m ² /g)	H ₂ Uptake (mmol/g)		Crystallite Size (nm)
	CeO ₂	Pt	Re		Exp.	Theor.	
CeO ₂	-	-	-	175	-	-	6.10
W1 (2Pt/1Re/CeO ₂)	99.12	0.59	0.29	171	0.63	0.13	6.09
W2 (1Pt/1Re/CeO ₂)	99.10	0.45	0.45	169	0.84	0.15	6.05
W3 (1Pt/2Re/CeO ₂)	99.11	0.30	0.59	168	0.84	0.16	6.15

All the XRD diffractograms of the powder catalysts displayed the cubic fluorite-type for CeO₂ crystal phase [26], and no diffraction peaks corresponding to Pt, Re or the corresponding oxides phase could be identified, due to the low loading and high dispersion of the noble metal phases (Figure 1). Moreover, the calculation of the crystallite sizes by means of the Scherrer equation demonstrates that active species deposition had no effect on the dimension of ceria crystallites (Table 1). For ceria and its solid solutions, Raman spectroscopy contributes to the improved understanding of local structural changes in the nearest and next nearest neighbor shells of Pt and Re dopant cations and oxygen vacancies. Raman is an excellent tool to investigate the defect chemistry of doped and un-doped ceria, due to its sensitivity to non-periodic features. The Raman spectrum of ceria support (Figure 2) showed the typical strong peak at 464 cm⁻¹ attributed to the first order F_{2g} mode [27] (Ce⁴⁺-O-Ce⁴⁺ wagging) and the barely visible broad peaks at 258, 595 and 1,179 cm⁻¹, respectively attributed to second-order transverse acoustic (2TA), defect-induced (D) (recently demonstrated to be Ce³⁺-O-Ce⁴⁺ stretching [28]) and second-order longitudinal optical modes (2LO) [29]. The Raman spectrum of the W1 catalyst (Pt/Re ratio 2/1) still showed the peak of the first order F_{2g} mode, but instead of D transition, two broad peaks at 575 cm⁻¹ and 657 cm⁻¹ were visible, attributed to the interaction of Pt with the cerium oxide surface [30]. Moreover, at 829 cm⁻¹, a small peak attributed to the antisymmetric stretching mode of Re-O-Re appeared [31].

The Raman spectrum of the W2 catalyst (Pt/Re ratio 1/1) still showed the peak ascribable to the first order F_{2g} mode; regarding the two broad peaks at 575 cm⁻¹ and 657 cm⁻¹, attributed in W1 to the interaction of Pt with cerium oxide surface appeared, the latter seemed to disappear. On the contrary, a further peak was observed at 982 cm⁻¹, which is due to symmetric Re-O stretching [31]. For the W3 catalyst (Pt/Re ratio 1/2), two peaks attributed to Re-O stretching can be observed in the Raman spectrum, while the two broad peaks at 575 cm⁻¹ and 657 cm⁻¹, ascribed to the interaction of Pt with cerium oxide surface for the sample W1, disappeared and a new peak at 595 cm⁻¹ was observed, linked to defect-induced (D) in ceria. These results suggested that the interaction of platinum with ceria mainly occurs at the D sites. TEM images showed the morphology of the catalysts, suggesting a single phase of spherical type (Figure 3), moreover, the particle size agreed with the crystallite size, calculated

by the Scherrer equation. However, the black area may represent groups of accumulated particles. The temperature programmed reduction (TPR) profiles of the three catalysts can be divided in two main areas. The broad peak between 700 K and 750 K was attributed to ceria's surface reduction [32] (Figure 4). The peaks between 500 K and 600 K are ascribable to an overlapping of three reduction peaks of PtOx and ReOx species and the ceria surface, as the result of the spillover effect from metal particles to the support [33].

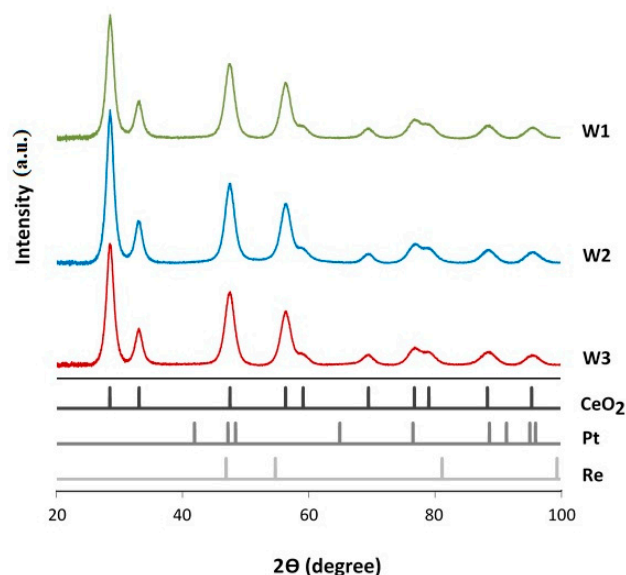


Figure 1. Diffractograms of powder catalysts: W1, W2 and W3.

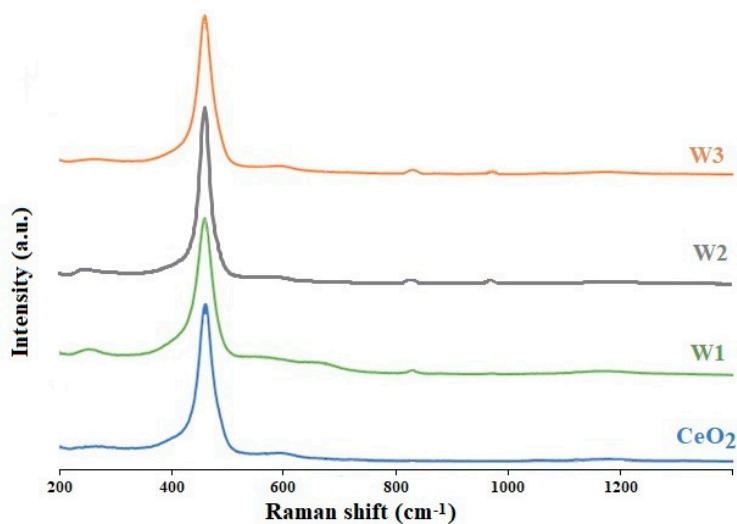


Figure 2. Raman spectra of ceria and powder catalysts: W1, W2 and W3.

Specifically, the TPR profile of W1 catalyst showed a perfect overlapping, with the peak centered at 550 K, while in the case of W2 and W3 TPR profiles, the main peak shifted respectively to 593 K and 608 K, and a shoulder on the left appeared in both the curves, centered between 505 K and 510 K.

These results suggest a correlation between the temperature of the main reduction peak and the Pt/Re ratio, suggesting a strong interaction between platinum and rhenium. The evaluation of hydrogen uptake, calculated by integrating the H₂-TPR profiles, as expected, confirmed the advent of the spillover phenomenon; in fact, the hydrogen consumed in each experiment was more than one order of magnitude higher compared to the expected value (Table 1).

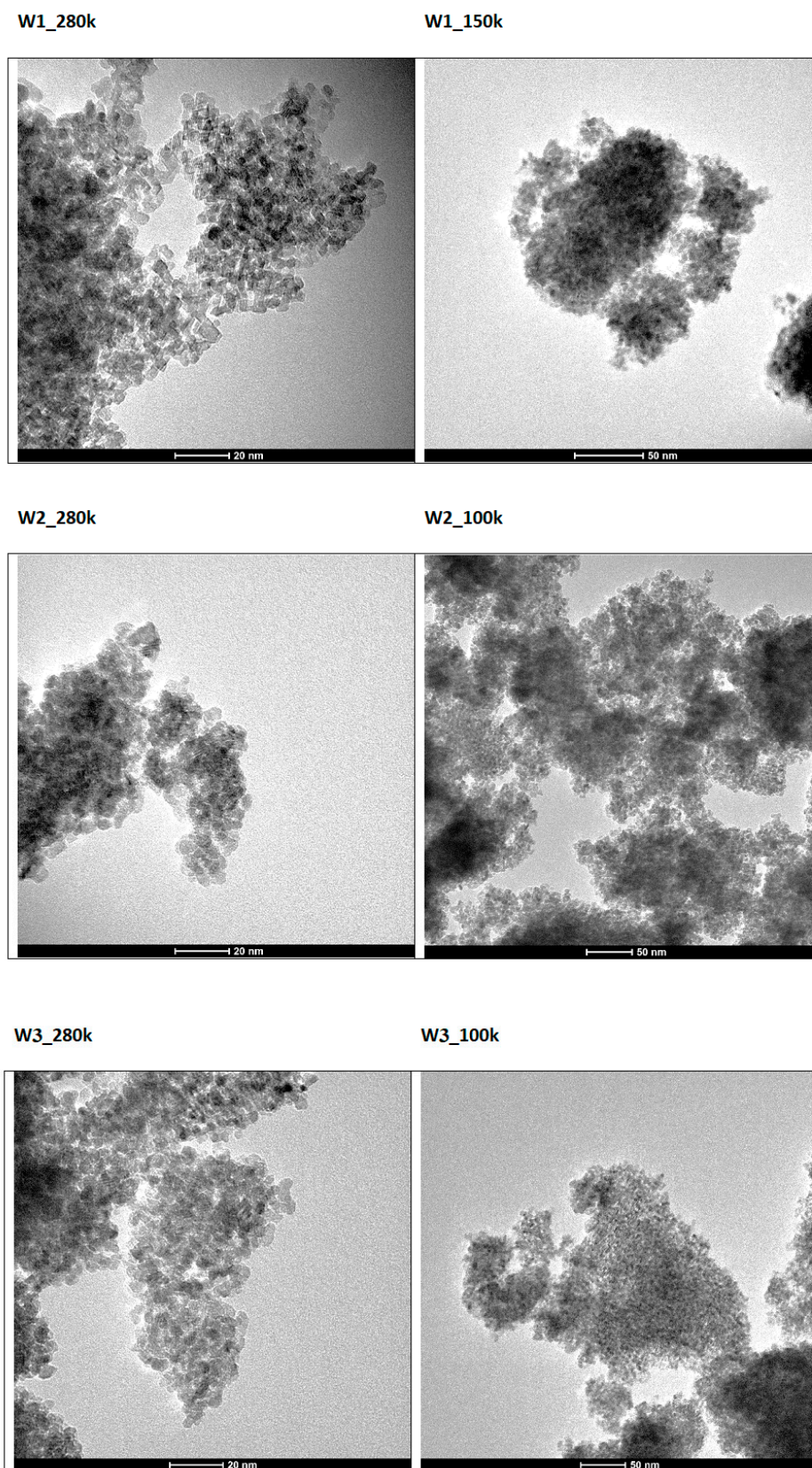


Figure 3. Transmission electron microscopy (TEM) images of powder catalysts: W1, W2 and W3.

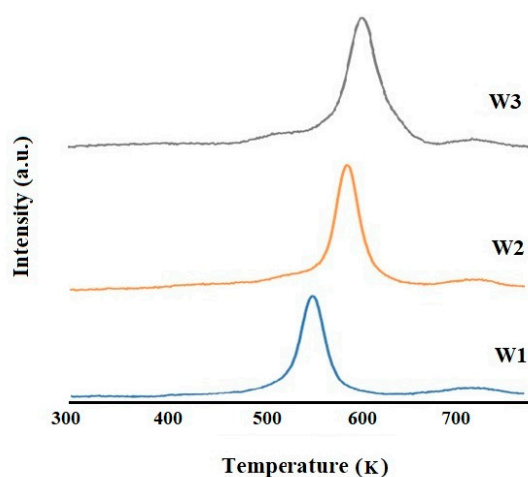


Figure 4. Temperature programmed reduction with hydrogen (H_2 -TPR) of powder the catalysts: W1, W2 and W3.

2.1.2. Activity Tests

Figure 5a–c shows the catalytic activity of the three investigated catalysts towards the WGS reaction between 500 and 600 K as a function of the steam to carbon monoxide ratio. In Figure 5d the results obtained at the same H_2O/CO ratio (24/7) are compared.

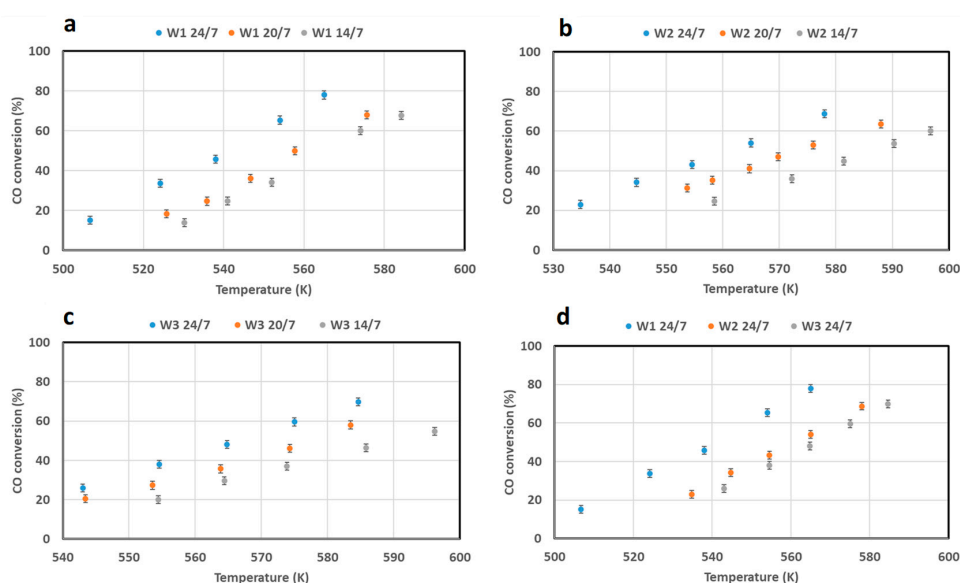


Figure 5. CO conversion as function of temperature for different H_2O/CO ratio (24/7, 20/7, 14/7) for each powder catalyst: W1 (a), W2 (b) and W3 (c), and CO conversion comparison as function of the temperature at the same H_2O/CO ratio (24/7) for the three catalysts (d). $\tau = 131$ ms.

As expected, the increase in the H_2O/CO ratio favored the WGS reaction for all the three catalysts. In particular, for the W1 sample, the variation of the H_2O/CO ratio from 20/7 to 24/7 resulted in a more pronounced improvement of the catalytic activity, with the profiles achieved for $H_2O/CO=20/7$ and 14/7 closer. For the other two catalysts, by changing the feeding conditions, such a strong enhancement in CO conversion was not observed. Moreover, at a fixed H_2O/CO ratio of 24/7, the W1 catalyst showed higher CO conversion than the W2 and W3 catalysts, which essentially displayed similar activity. For example, at 565 K, the W1 reached a conversion of almost 80%, while for the other two samples a value around 50% was recorded. These results demonstrated that the catalyst with a Pt/Re ratio equal to 2/1 is more active than the catalysts with the Pt/Re ratio equal to 1/1 and 1/2.

This trend seems to suggest a direct correlation with the reduction temperature of the PtO_x/ReO_y system in the H₂-TPR experiments and thus with Pt/Re loading and the catalytic activity. The 2Pt/1Re catalyst, in fact, displayed lower reduction temperatures compared to the other two samples and the strong correlation between the easy reducibility and the activity for WGS was already reported for CeO₂-based catalysts [34]. The most active formulation was deposited on a foam structured carrier and further tested.

2.1.3. Kinetic Measurements

The experimental results obtained over the three Pt/Re catalysts and the analysis of product distribution as a function of reaction temperature, particularly regarding the methane formation, suggested that the reaction pathway over the three Pt/Re catalysts involved water–gas shift reactions and both CO as well as CO₂ methanation. The pre-exponential factors and the apparent activation energies estimated for the three above reactions from the Arrhenius plots over the W1, W2 and W3 sample are shown in Table 2. The kinetic model results were validated by comparing them with the experimental results. In Figure 6, as an example, the comparison related to three catalytic systems in the condition of H₂O/CO = 14/7 is reported. The data showed a good agreement between the kinetic model and the experimental results; in particular, it is possible to highlight that the kinetic model was able to predict the behavior of the catalytic systems in the investigated temperature range and, more importantly, it was able—fixing the active species ratio—to take into account the variation of the different feeding conditions investigated in this work (H₂O/CO ratio in the range 2–3.84). The activation energy calculated for the W2 and W3 catalysts, with Pt/Re ratio of 1/1 and 1/2 respectively, were very close, both for WGS reaction and CO and CO₂ methanation.

Table 2. Kinetic parameters for the powder catalysts.

	W1	W2	W3
$k_{0, \text{WGS}}$ (mol/(g·min·atm ²))	1608326	1225116014	1225116014
$E_{a, \text{WGS}}$ (kJ/mol)	78	114	118
$k_{0, \text{CO}}$ (mol/(g·min·atm ²))	2989	40000	40000
$E_{a, \text{CO}}$ (kJ/mol)	94	85	85
k_{0, CO_2} (mol/(g·min·atm ²))	0.00712	6.9	6.9
E_{a, CO_2} (kJ/mol)	16	50	48

On the other hand, the activation energy for the W1 catalyst, with a Pt/Re ratio of 2/1, of WGS reaction was much lower and the CO methanation was higher, suggesting a preference for the WGS reaction. Thus, the results shown in Table 2 confirmed the improved activity of the 2Pt-1Re/CeO₂ catalyst for the water–gas shift reaction (discussed in Paragraph 2.1.2), with an E_a of about 78 kJ/mol: the easier reducibility assured an enhancement in catalyst activity compared to the W2 and W3 samples, which displayed WGS activation energies of 114 and 118 kJ/mol, respectively. The found values agreed well with kinetic data reported in the literature for similar catalytic formulations [35].

2.2. Structured Catalyst

2.2.1. Characterization Results

The structured catalyst (denoted as S1) was prepared by coating the commercial aluminum alloy foams, with a relative density of 25%, by means of chemical conversion coating, with cerium oxide. The chemical conversion coating technique is traditionally used in protecting aluminum alloys from corrosion [36], and recently it has been successfully used in catalysis [37]. This technique presents many advantages with respect to the washcoating [38] (the most widely used technique to prepare structured catalysts), including the high resistance to the mechanical stress of the coating, and the usability with highly porous structures, for which the washcoating might occlude the pores. The active

components were loaded by wet impregnation with rhenium and platinum precursors. The ED-XRF analysis showed that the total loading of the catalytic formulation on the foams was on average 5.1 wt%, and the Pt/Re ratio was equal to 1.9 (Table 3).

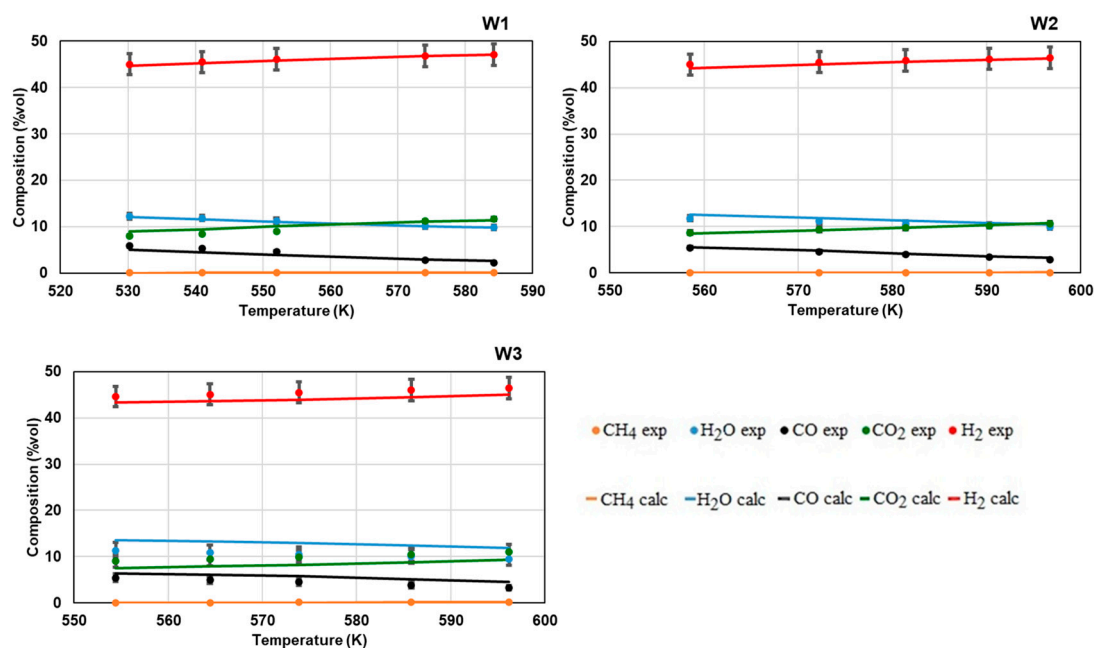


Figure 6. Comparison of the experimental results and the kinetic model results for the three catalytic systems, in the condition $H_2O/CO = 14/7$.

Table 3. Structured catalyst characterization.

	Catalytic Formulation		SSA _{B.E.T.} (m ² /g)	H ₂ Uptake (mmol/g)		Relative Density (%)
	Loading (wt%)	Pt/Re Ratio		Exp.	Theor.	
Al-foam	-	-	1	-	-	25
S1	5.1	1.9	3.8	1.2	0.13	-

The specific surface area measurements on the structured catalyst showed an increase of the surface area of the structure due to the ceria coating loading; on the basis of the result, a surface area between 70 m²/g and 80 m²/g for the ceria coating was hypothesized.

The hydrogen uptake measured during the TPR experiments was one order of magnitude higher than the theoretical one (Table 3), due to the spillover effect, however, the extension of this phenomenon was higher than in the case of the powder catalyst with the same Pt/Re ratio (Table 1). The H₂-TPR profile of the structured catalyst was very different from the profile of the powder catalyst with the same Pt/Re ratio (Figure 7). The case of the powder catalyst's two main peaks was present, however, the first peak was centered at a lower temperature, while the second peak showed a higher relative intensity, attributed to a much higher reducibility of the ceria surface, in agreement with the higher hydrogen measured uptake. These results suggested a different oxygen storage capacity of the ceria coating [39], attributable mainly to the preparation technique. In Figure 8, the scanning electron microscopy (SEM) images at different magnification of the structured catalyst S1 are showed (a, c), with the intent to highlight the surface morphology. As is evident, the catalyst surface is extremely irregular, with the presence of numerous cavities and fractures, which justify the increase in surface area obtained due to the coating, and which are beneficial for the catalytic activity.

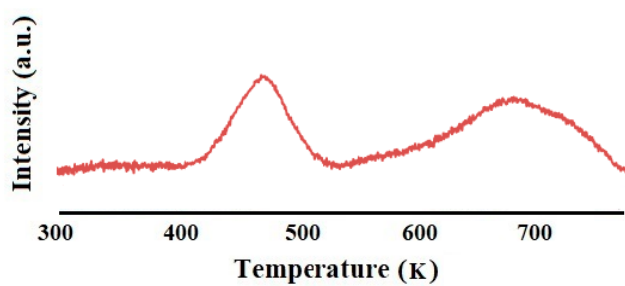


Figure 7. H₂-TPR of the structured catalyst.

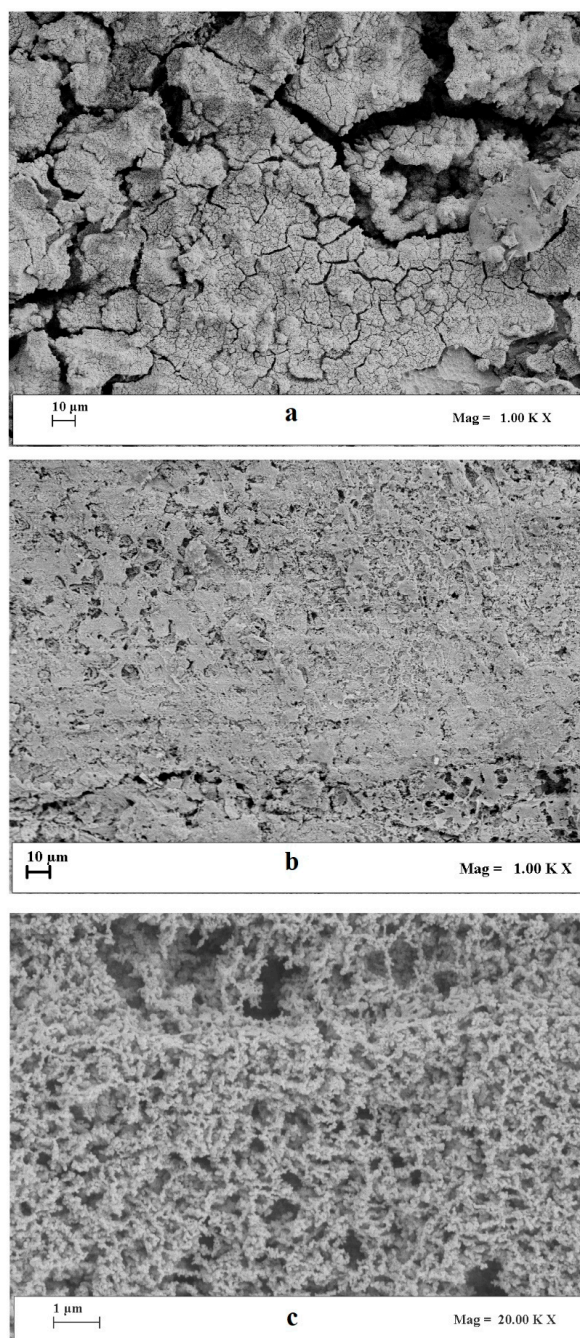


Figure 8. SEM (scanning electron microscopy) image of S1 structured catalyst at different magnitude (a,c), and a SEM image of a structured catalyst obtained by washcoating and loaded with Pt/Re/CeZrO₄ catalytic formulation (b).

Moreover, the nanometric nature of the coating is highlighted if compared with the SEM image of a structured catalyst obtained by washcoating (Figure 8b), prepared in previous work, with a similar catalytic formulation (1Pt/1Re/CeZrO₄) [8].

2.2.2. Kinetic Measurements

The results of the kinetic study performed on the structured catalysts are summarized in Table 4 in terms of pre-exponential factor and activation energy.

Table 4. Kinetic parameters for the structured catalyst.

	k_0 (mol/(g·min·atm ²))	Ea (kJ/mol)
r_{WGS}	1608326	80
r_{CO}	2500	85
r_{CO_2}	1000	75

The kinetic model results were validated by comparing them with the experimental results. In Figure 9, the comparison related to the structured catalyst in the condition of H₂O/CO = 24/7 is reported.

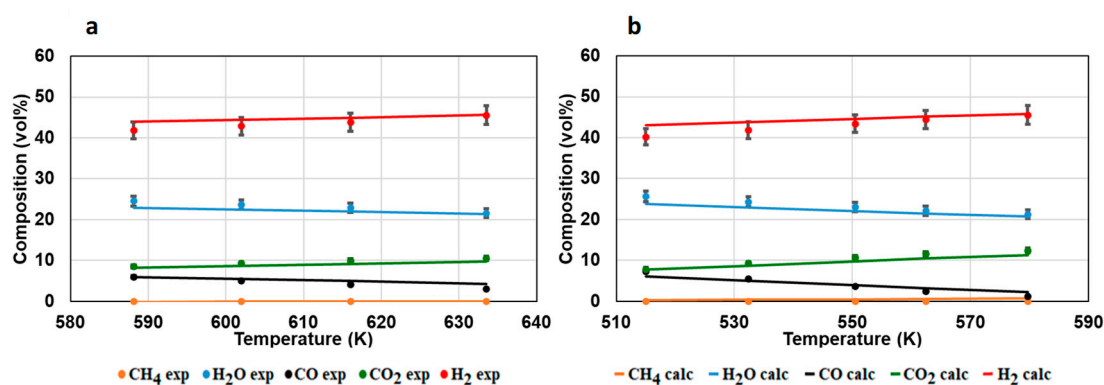


Figure 9. Comparison of the experimental results and the kinetic model results for the structured catalyst, in the condition H₂O/CO = 24/7, at two different contact times, 23 ms (a) and 131 ms (b).

The data shown in Figure 9 evidence a good agreement between the predicted values and the experimental results, thus demonstrating the feasibility of the kinetic model. The comparison of the kinetic parameters related to the structured (Table 4) and powder catalyst W1 (Table 2) evidenced that the two catalytic systems were characterized by very similar values of the pre-exponential factor and activation energy for WGS, but they had different values regarding the methanation parameters. This result suggested that the two catalytic systems were different, due to the preparation technique, as was also confirmed by the TPR results. However, it is worthwhile noting that, as described above for the powder sample, the activation energy of the WGS is lower than the methanation ones, therefore evidencing a preference for the WGS reaction.

2.2.3. Activity Tests

The activity tests on the structured catalyst were carried out with the aim of testing the feasibility of a single stage WGS process, evaluating the performance for intermediate temperatures with a simulated syngas mixture feeding at a target contact time. In Figure 10a, the CO conversion as a function of the temperature, at three different contact times ($\tau = 23, 79$ and 131 ms) and for a H₂O/CO ratio = 24/7, is shown. The test carried out at 131 ms showed comparable activity with respect to the corresponding powder catalyst, the test were performed at 23 ms, although under a space velocity of

more than five times higher compared to the value selected for the powder sample, showed satisfactory results, with a CO conversion of almost 60% at 635 K (Figure 10a).

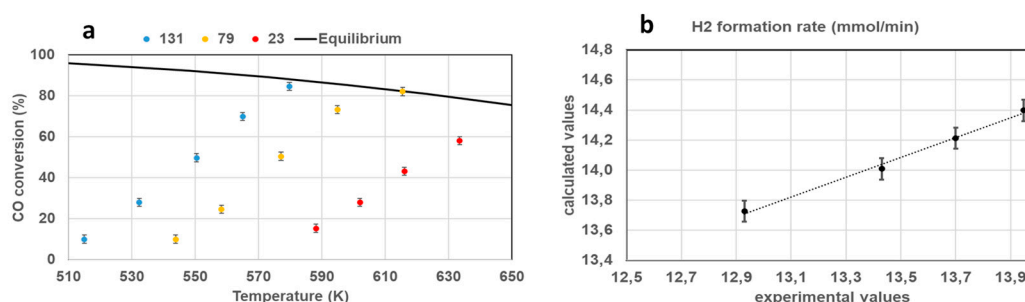


Figure 10. CO conversion as function of temperature (a) and comparison between hydrogen formation rate experimental vs. calculated values (b) for S1 catalyst with a $\text{H}_2\text{O}/\text{CO} = 24/7$, at a $\tau = 23$ ms.

The experimental hydrogen formation rate was also evaluated, highlighting once again a good agreement with the values predicted by the model (Figure 10b). The structured catalyst was also tested under a simulated reformat gas mixture coming from an ethanol pre-reformer followed by a methane reforming unit [40]. The catalyst activity was investigated in the temperature range 540–690 K and the results, showed in Figure 11, are presented in terms of CO conversion (a) and product gas distribution as a function of outlet reaction temperature (b). CO conversion linearly increased up to 610 K, showing a decreasing trend above 630 K; due to the negative effect of high temperatures on WGS thermodynamics. Only slight variations in methane concentration with reaction temperature were observed, suggesting that carbon oxide methanation was not the dominant pathway under the investigated conditions. A hydrogen production rate of 18.7 mmol/min was recorded at 685 K and this value (properly scaled on the basis of the different feeding flow-rates) was compared with the results of the simulations performed. The hydrogen productivity recorded over the structured catalyst is only 14% lower than the value reported, and this difference is mainly ascribable to the employment of a membrane in the WGS reactor in the reference process scheme. These very promising results allow us to conclude that the S1 structured catalyst is a suitable sample for the realization of a single-stage WGS process.

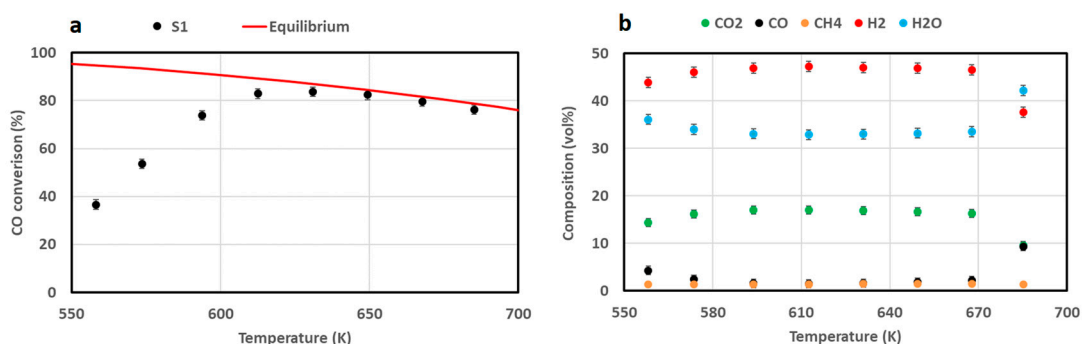


Figure 11. CO conversion (a) and product gas distribution as a function of reaction temperature (b) for S1 catalyst under a simulated reformat gas (37.61 vol% H_2 , 9.31 vol% CO_2 , 9.31 vol% CO , 42.19 vol% H_2O , 1.37 vol% CH_4), $\tau = 53$ ms.

3. Materials and Methods

3.1. Powder Catalysts Preparation

The powder catalysts were prepared by sequential dry impregnation of Actalys HSA commercial ceria, with the rhenium and platinum precursors respectively, with a total loading of platinum and rhenium equal to 1 wt% with respect to the total weight of the catalyst. Three catalysts with a variable

platinum/rhenium ratio of 2/1, 1/1 and 1/2 were prepared. The porous volume of the ceria was measured by mixing 5 g of support with the minimum amount of distilled water needed, then the support was dried at 393 K for 2 h and impregnated with an ammonium perrhenate solution, obtained by dissolving the desired amount of the rhenium salt in a volume of water corresponding to the porous volume of the ceria. The obtained mixture was dried at a temperature of 343 K for 16 h and calcined at 773 K for 1 h. The resulting solid was treated as previously described, in order to evaluate its porous volume, then dried at 393 K for 2 h and impregnated with a solution of tetraamineplatinum (II) nitrate, obtained by dissolving the desired amount of the platinum salt in a volume of water corresponding to the porous volume previously measured. The obtained mixture was dried at a temperature of 343 K for 16 h and calcined at 773 K for 1 h.

3.2. Structured Catalyst Preparation

The structure was obtained by assembly 7 circular open cell aluminum alloy foams with a diameter of 1.4 cm, obtained by cutting and shaping 1 cm thick commercial sheet. The as obtained foams were cleaned and corroded by treating with 5 vol% HF solution for 4 min, then washed with distilled water and dried at 393 K for 2 h. The ceria coating was realized by means of chemical conversion coating described in a previous article [41]. The corroded foams were degreased with a 5 wt% solution of NaOH for one minute, washed with distilled water, then etched in a 35 vol% solution of HNO₃, washed with distilled water, then treated with a chemical bath to coating the surface with ceria support. The coating bath consisted of an acidic solution (pH = 2, by HCl) obtained by dissolving CeCl₃·7H₂O (1.3 wt%), 35% wt H₂O₂ (3.8 wt%) in distilled water. The foams were treated with this solution for 2 h at 328 K; the treatment was repeated three times. After each treatment, the reacted foams were washed with distilled water and dried for 2 h at 393 K. After the third treatment the foams were calcined at 773 K for 1 h. Rhenium and platinum were loaded by wet impregnation of the coated structures, by immersing in the metal salt precursor solution at 328 K for 20 min, followed by drying at 393 K for 2 h and calcining at 773 K for 1 h.

3.3. Catalysts Characterization

The catalysts were characterized with a series of physical–chemical analytical techniques. The B.E.T. specific surface areas measurements were carried out with a Costech Sorptometer 1040 (Costech International, Milano, Italy), by dynamic N₂ adsorption at 77 K. The crystal phases were obtained by X-ray powder diffraction (Rigaku MiniFlex 600). The crystallite sizes were calculated from the diffractograms by applying the Scherrer equation. The chemical composition was checked by means of an ARLTM QUANT'X ED-XRF spectrometer (Thermo Scientific, Rodano, Italy), while the structural features were evaluated with a Raman spectroscopy using an inVia Raman Microscope (Renishaw, Pianezza, Italy), equipped with a 514 nm Ar ion laser operating at 25 mW. TEM images were obtained with a FEI Tecnai 20 (Sphera) microscopy operating at 200 kV LaB6 filament. Samples morphology was observed by a Field Emission Scanning Electron Microscope (FE-SEM, mod. LEO 1525, Carl Zeiss SMT AG, Oberkochen, Germany). The H₂-TPR experiments were carried out in the temperature range of 293–723 K, with a reducing stream of 500 Ncc/min containing 5 vol% of H₂ in Ar, applying a heating rate of 10 K/min, in the same reactor used for the activity tests, as described below.

3.4. Catalytic Activity Tests

The powder catalysts were previously compacted and sieved in the 180–355 μm range and diluted with quartz glass at the same total volume. The activity tests were carried out on the reduced catalysts, at atmospheric pressure, in the temperature range 500–620 K, at a contact time $\tau_c = 131$ ms, with a reacting mixture 43 vol% H₂, 7 vol% CO₂, 7 vol% CO, X vol% H₂O (X = 14, 20 or 24), balance Argon. The structured catalyst was surrounded by a thermo expanding pad with a thickness of 3 mm, and previously reduced in the H₂-TPR experiments. The activity tests were carried out at atmospheric pressure, in the temperature range 500–620 K, at a contact time range $\tau_c = 23$ –131 ms,

with two different reacting mixture, the first was 43 vol% H₂, 7 vol% CO₂, 7 vol% CO, 24 vol% H₂O, 19 vol% Argon, the second was 37.61 vol% H₂, 9.31 vol% CO₂, 9.31 vol% CO, 42.19 vol% H₂O, 1.37 vol% CH₄. The catalytic activity tests were performed in a stainless-steel tubular reactor with an internal diameter of 22 mm and a length of 40 cm. The reaction products were dried through a refrigerator Julabo F12 (JULABO Labortechnik GmbH77960 Seelbach, Germany) and sent to a Hiden Analytical mass spectrometer (Hiden Analytical, 420 Europa Blvd, Westbrook, Warrington WA5 7 UN, UK).

3.5. Kinetic Measurements

The kinetic evaluation was performed by numerically analyzing the results of dedicated experimental tests, carried out at atmospheric pressure using mixtures of CO, CO₂, H₂, H₂O, and Ar. The tests were performed as described in the previous paragraph, by varying the H₂O/CO ratio in a wide temperature range. In particular, the data regarding the catalytic performance of the system far from the thermodynamic equilibrium conditions were considered, so that differential reaction conditions could be assumed, with negligible heat and mass transfer effects. The approach described below was followed both for the powder and for the structured catalysts, even if for the structured catalyst only the operating condition corresponding to the H₂O/CO ratio = 24/7 (the condition in which the powder catalyst showed the best catalytic performance) was analyzed.

The reactions used for the numeric analysis are:

- The WGS reaction: $\text{CO} + \text{H}_2\text{O} = \text{CO}_2 + \text{H}_2$
- The CO methanation: $\text{CO} + 3\text{H}_2 = \text{CH}_4 + \text{H}_2\text{O}$
- The CO₂ methanation: $\text{CO}_2 + 4\text{H}_2 = \text{CH}_4 + 2\text{H}_2\text{O}$

The reaction rates of the above reported reactions were expressed as follows, considering that (i) for the WGS reaction the k_{eq} was calculated using the expression proposed by Moe [42], and (ii) for the two methanation reactions a kinetic expression based on a Langmuir–Hinshelwood approach was used:

- $-r_{\text{CO}} = k_{\text{WGS}} \left(P_{\text{CO}} P_{\text{H}_2\text{O}} - \frac{P_{\text{CO}_2} P_{\text{H}_2}}{k_{eq, \text{WGS}}} \right)$ with $k_{eq, \text{WGS}} = e^{\frac{4577.8}{T} - 4.33}$
- $-r_{\text{CO}} = k_{\text{CO}} \frac{P_{\text{CO}} P_{\text{H}_2}}{(1 + K_{\text{CO}} P_{\text{CO}} + K_{\text{H}_2\text{O}} P_{\text{H}_2\text{O}})^2}$
- $-r_{\text{CO}_2} = k_{\text{CO}_2} \frac{P_{\text{CO}_2} P_{\text{H}_2}}{(1 + K_{\text{CO}_2} P_{\text{CO}_2} + K_{\text{CO}} P_{\text{CO}} + K_{\text{H}_2\text{O}} P_{\text{H}_2\text{O}})^2}$

In the above reported expressions, the terms have the following meaning:

- P_i is the partial pressure of the component “i”.
- $k_i(T)$ is the reaction rate constant according to the Arrhenius law: $k_i = k_{0,i} e^{-\frac{E_{A,i}}{RT}}$, with $k_{0,i}$ = pre-exponential factor and $E_{A,i}$ = the activation energy.
- $K_j(T)$ are the adsorption constants for the component “j”, expressed according to the Arrhenius law [41]: $K_j = K_{0,j} e^{-\frac{H_{A,j}}{RT}}$, with $K_{0,j}$ = pre-exponential factor and $\Delta H_{A,j}$ = the adsorption heat.

The material balances on the single components allowed obtaining a set of equations, resolved by applying the Euler method by means of the Excel software. For each operating condition, the experimental results were compared with the one from the kinetic model, and the Solver of the Excel software allowed the minimization of the function $f = \min \left(\sum_{c=1}^n (x_{exp,c} - x_{mod,c})^2 \right)$. The optimization procedure was performed several times with various initial values of the parameters, with the aim to confirm the robustness of the optimization scheme.

4. Conclusions

In this work, a comparative study on Pt/Re/CeO₂ powder catalysts, for CO water-gas shift reaction, has been presented. The activity of three catalysts, obtained by sequential dry impregnation of

commercial ceria with the salts precursors of rhenium and platinum, has been evaluated in water–gas shift reaction, as function of the temperature, of the Pt/Re ratio and of the feeding conditions (H₂O/CO ratio). The kinetic parameters have been calculated by means of numerical analysis, considering the water–gas reaction and CO and CO₂ methanation reactions. The results of the activity tests showed the best performance of catalyst with Pt/Re ratio equal to 2/1, which was related to the reduction temperature of the PtOx/ReOy system, observed in the H₂-TPR experiments. This catalyst showed lower reduction temperatures compared to the catalysts with Pt/Re ratio equal to 1/1 and 1/2. In the second part of the work a structured catalyst, loaded with the 2Pt/1Re/CeO₂ catalytic formulation, has been prepared, by coating with ceria a commercial alumina alloy foam by means of chemical conversion coating technique. The SEM images highlighted the nanometric structure and the high rough of the coating. The catalytic activity tests and the kinetic evaluation have been showed a good scale up of the performance from the powder to the structured catalyst. Moreover, the catalytic activity of the structured catalyst has been evaluated in simulated reformat gas feeding conditions, showing that is possible to design a single-stage WGS process, with the prepared structured catalyst.

Author Contributions: Conceptualization, V.P. and M.M.; methodology, V.P., P.P., C.R., E.M. and M.M.; investigation, V.P., F.G., P.P., C.R., E.M. and M.M.; data curation, C.R., E.M. and M.M.; writing—original draft preparation, C.R., E.M. and M.M.; writing—review and editing, V.P., F.G., P.P., C.R., E.M. and M.M.; supervision, V.P.; funding acquisition, V.P., F.G., P.P. All authors have read and agreed to the published version of the manuscript.

Funding: This work has received funding from the European Union’s Horizon 2020 research and innovation programme under the Marie Skłodowska-Curie grant agreement No 734561.

Acknowledgments: The authors wish to acknowledge Mariarosa Scognamiglio (Department of Industrial Engineering, University of Salerno) for SEM analysis, and Ing. Giovanni Festa for the valuable contribution.

Conflicts of Interest: The authors declare no conflict of interest.

References

1. Palma, V.; Ruocco, C.; Cortese, M.; Martino, M. Recent Advances in Structured Catalysts Preparation and Use in Water-Gas Shift Reaction. *Catalysts* **2019**, *9*, 991. [[CrossRef](#)]
2. Lee, D.-W.; Lee, M.S.; Lee, J.Y.; Kim, S.; Eom, H.-J.; Moon, D.J.; Lee, K.-Y. The review of Cr-free Fe-based catalysts for high-temperature water-gas shift reactions. *Catal. Today* **2013**, *210*, 2–9. [[CrossRef](#)]
3. Uchida, H.; Isogai, N.; Oba, M.; Hasegawa, T. The zinc oxide copper catalyst for carbon monoxide-shift conversion. I. The dependency of the catalytic activity on the chemical composition of the catalyst. *Bull. Chem. Soc. Jpn.* **1967**, *40*, 1981–1986. [[CrossRef](#)]
4. Cifuentes, B.; Bustamante, F.; Cobo, M. Single and Dual Metal Oxides as Promising Supports for Carbon Monoxide Removal from an Actual Syngas: The Crucial Role of Support on the Selectivity of the Au–Cu System. *Catalysts* **2019**, *9*, 852. [[CrossRef](#)]
5. Palma, V.; Pisano, D.; Martino, M. CFD modeling of the influence of carrier thermal conductivity for structured catalysts in the WGS reaction. *Chem. Eng. Sci.* **2018**, *178*, 1–11. [[CrossRef](#)]
6. Van Dijk, H.A.J.; Boon, J.; Nyqvist, R.N.; Van Den Brink, R.W. Development of a single stage heat integrated water-gas shift reactor for fuel processing. *Chem. Eng. J.* **2010**, *159*, 182–189. [[CrossRef](#)]
7. Palma, V.; Pisano, D.; Martino, M.; Ricca, A.; Ciambelli, P. High Thermal Conductivity Structured Carriers for Catalytic Processes Intensification. *Chem. Eng. Trans.* **2015**, *43*, 2047–2052. [[CrossRef](#)]
8. Palma, V.; Pisano, D.; Martino, M. Structured noble metal-based catalysts for the WGS process intensification. *Int. J. Hydrog. Energy* **2018**, *43*, 11745–11754. [[CrossRef](#)]
9. Stiegler, T.; Meltzer, K.; Tremel, A.; Baldauf, M.; Wasserscheid, P.; Albert, J. Development of a Structured Reactor System for CO₂ Methanation under Dynamic Operating Conditions. *Energy Technol.* **2019**, *7*, 1900047. [[CrossRef](#)]
10. Palma, V.; Pisano, D.; Martino, M. Comparative Study Between Aluminum Monolith and Foam as Carriers for The Intensification of The CO Water Gas Shift Process. *Catalysts* **2018**, *8*, 489. [[CrossRef](#)]

11. Kam, R.; Scott, J.; Amal, R.; Selomulya, C. Pyrophoricity and stability of copper and platinum based water-gas shift catalysts during oxidative shut-down/start-up operation. *Chem. Eng. Sci.* **2010**, *65*, 6461–6467. [[CrossRef](#)]
12. Zhu, M.; Wachs, I.E. Iron-Based Catalysts for the High-Temperature Water-Gas Shift (HTWGS) Reaction: A Review. *ACS Catal.* **2016**, *6*, 722–732. [[CrossRef](#)]
13. Ruettinger, W.; Ilinich, O.; Farrauto, R.J. A new generation of water gas shift catalysts for fuel cell applications. *J. Power Sources* **2003**, *118*, 61–65. [[CrossRef](#)]
14. Panagiotopoulou, P.; Kondarides, D.I. Effect of the nature of the support on the catalytic performance of noble metal catalysts for the water–gas shift reaction. *Catal. Today* **2008**, *112*, 49–52. [[CrossRef](#)]
15. de León, J.N.D.; Loera-Serna, S.; Zepeda, T.A.; Domínguez, D.; Pawelec, B.; Venezia, A.M.; Fuentes-Moyado, S. Noble metals supported on binary γ -Al₂O₃- α -Ga₂O₃ oxide as potential low temperature water-gas shift catalysts. *Fuel* **2020**, *266*, 117031. [[CrossRef](#)]
16. Chein, R.Y.; Lin, Y.H.; Chen, Y.C.; Chyou, Y.P.; Chung, J.N. Study on water-gas shift reaction performance using Pt-based catalysts at high temperatures. *Int. J. Hydrog. Energy* **2014**, *39*, 18854–18862. [[CrossRef](#)]
17. Castaño, M.G.; Reina, T.R.; Ivanova, S.; Centeno, M.A.; Odriozola, J.A. Pt vs. Au in water–gas shift reaction. *J. Catal.* **2014**, *314*, 1–9. [[CrossRef](#)]
18. Palma, V.; Martino, M. Pt-Re Based Catalysts for the Realization of a Single Stage Water Gas Shift Process. *Chem. Eng. Trans.* **2017**, *57*, 1657–1662. [[CrossRef](#)]
19. Sato, Y.; Terada, K.; Hasegawa, S.; Miyao, T.; Naito, S. Mechanistic study of water–gas-shift reaction over TiO₂ supported Pt–Re and Pd–Re catalysts. *Appl. Cat. A-Gen.* **2005**, *296*, 80–89. [[CrossRef](#)]
20. Carrasquillo-Flores, R.; Gallo, J.M.R.; Hahn, K.; Dumesic, J.A.; Mavrikakis, M. Density Functional Theory and Reaction Kinetics Studies of the Water–Gas Shift Reaction on Pt–Re Catalysts. *ChemCatChem* **2013**, *5*, 3690–3699. [[CrossRef](#)]
21. Iida, H.; Igarashi, A. Structure characterization of Pt-Re/TiO₂ (rutile) and Pt-Re/ZrO₂ catalysts for water gas shift reaction at low-temperature. *Appl. Cat. A-Gen.* **2006**, *303*, 192–198. [[CrossRef](#)]
22. Choung, S.Y.; Ferrandon, M.; Krause, T. Pt-Re bimetallic supported on CeO₂-ZrO₂ mixed oxides as water–gas shift catalysts. *Catal. Today* **2005**, *99*, 257–262. [[CrossRef](#)]
23. Sato, Y.; Terada, K.; Soma, Y.; Miyao, T.; Naito, S. Marked addition effect of Re upon the water gas shift reaction over TiO₂ supported Pt, Pd and Ir catalysts. *Catal. Commun.* **2006**, *7*, 91–95. [[CrossRef](#)]
24. Azzam, K.G.; Babich, I.V.; Seshan, K.; Lefferts, L. Role of Re in Pt–Re/TiO₂ catalyst for water gas shift reaction: A mechanistic and kinetic study. *Appl. Cat. B-Environ.* **2008**, *80*, 129–140. [[CrossRef](#)]
25. del Villar, V.; Barrio, L.; Helmi, A.; Van Sint Annaland, M.; Gallucci, F.; Fierro, J.L.G.; Navarro, R.M. Effect of Re addition on the WGS activity and stability of Pt/CeO₂-TiO₂ catalyst for membrane reactor applications. *Catal. Today* **2016**, *268*, 95–102. [[CrossRef](#)]
26. Palma, V.; Ruocco, C.; Meloni, E.; Ricca, A. Renewable Hydrogen from Ethanol Reforming over CeO₂-SiO₂ Based Catalysts. *Catalysts* **2017**, *7*, 226. [[CrossRef](#)]
27. Cooper, A.; Davies, T.E.; Morgan, D.J.; Golunski, S.; Taylor, S.H. Influence of the Preparation Method of Ag-K/CeO₂-ZrO₂-Al₂O₃ Catalysts on Their Structure and Activity for the Simultaneous Removal of Soot and NOx. *Catalysts* **2020**, *10*, 294. [[CrossRef](#)]
28. Xu, Y.; Wang, F.; Liu, X.; Liu, Y.; Luo, M.; Teng, B.; Fan, M.; Liu, X. Resolving a Decade-Long Question of Oxygen Defects in Raman Spectra of Ceria-Based Catalysts at Atomic Level. *J. Phys. Chem. C* **2019**, *123*, 18889–18894. [[CrossRef](#)]
29. Wu, Z.; Li, M.; Howe, J.; Mayer III, H.M.; Overbury, S.H. Probing Defect Sites on CeO₂ Nanocrystals with Well-Defined Surface Planes by Raman Spectroscopy and O₂ Adsorption. *Langmuir* **2010**, *26*, 16595–16606. [[CrossRef](#)]
30. Brogan, M.S.; Dines, T.J.; Cairns, J.A. Raman spectroscopic study of the Pt-CeO₂ interaction in the Pt/Al₂O₃-CeO₂ catalyst. *J. Chem. Soc. Faraday Trans.* **1994**, *90*, 1461–1466. [[CrossRef](#)]
31. Hardcastle, F.D.; Wachs, I.E.; Horsley, J.A.; Via, G.H. The structure of surface rhenium oxide on alumina from laser raman spectroscopy and x-ray absorption near-edge spectroscopy. *J. Mol. Catal.* **1988**, *46*, 15–36. [[CrossRef](#)]
32. Rocchini, E.; Trovarelli, A.; Llorca, J.; Graham, G.W.; Weber, W.H.; Maciejewski, M.; Baiker, A. Relationships between Structural/Morphological Modifications and Oxygen Storage–Redox Behavior of Silica-Doped Ceria. *J. Catal.* **2000**, *194*, 461–478. [[CrossRef](#)]

33. Prins, R. Hydrogen spillover. Facts and fiction. *Chem. Rev.* **2012**, *112*, 2714–2738. [[CrossRef](#)]
34. Jeong, D.-W.; Potdar, H.S.; Shim, J.-O.; Jang, W.-J.; Roh, H.-S. H₂ production from a single stage water-gas shift reaction over Pt/CeO₂, Pt/ZrO₂, and Pt/Ce_(1-x)Zr_(x)O₂ catalysts. *Int. J. Hydrog. Energy* **2013**, *38*, 4502–4507. [[CrossRef](#)]
35. Radhakrishnan, R.; Willigan, R.R.; Dardas, Z.; Vanderspurt, T.H. Water gas shift activity and kinetics of Pt/Re catalysts supported on ceria-zirconia oxides. *Appl. Cat. B-Environ.* **2006**, *66*, 23–28. [[CrossRef](#)]
36. Dabalà, M.; Armelao, L.; Buchberger, A.; Calliari, I. Cerium-based conversion layers on aluminum alloys. *Appl. Surf. Sci.* **2001**, *172*, 312–322. [[CrossRef](#)]
37. Palma, V.; Goodall, R.; Thompson, A.; Ruocco, C.; Renda, S.; Leach, R.; Martino, M. Ceria-coated Replicated Aluminium Sponges as Catalysts for the CO-Water Gas Shift Process. *Int J. Hydrog. Energy* **2020**, in press. [[CrossRef](#)]
38. Cristiani, C.; Visconti, C.G.; Finocchio, E.; Gallo Stampino, P.; Forzatti, P. Towards the rationalization of the washcoating process conditions. *Catal. Today* **2009**, *147*, S24–S29. [[CrossRef](#)]
39. Lia, P.; Chen, X.; Li, Y.; Schwank, J.W. A review on oxygen storage capacity of CeO₂-based materials: Influence factors, measurement techniques, and applications in reactions related to catalytic automotive emissions control. *Catal. Today* **2019**, *327*, 90–115. [[CrossRef](#)]
40. Mosca, L.; Medrano Jimenez, J.A.; Assefa Wassie, S.; Gallucci, F.; Palo, E.; Colozzi, M.; Taraschi, S.; Galdieri, G. Process design for green hydrogen production. *Int. J. Hydrog. Energy* **2020**, *45*, 7266–7277. [[CrossRef](#)]
41. Palma, V.; Martino, M.; Truda, L. Nano-CeO₂ Coating on Aluminum Foam Carriers for Structured Catalysts Preparation. *Chem. Eng. Trans.* **2019**, *73*, 127–132. [[CrossRef](#)]
42. Ratnasamy, C.; Wagner, J. Water Gas Shift Catalysis. *Catal. Rev.-Sci. Eng.* **2009**, *51*, 325–440. [[CrossRef](#)]



© 2020 by the authors. Licensee MDPI, Basel, Switzerland. This article is an open access article distributed under the terms and conditions of the Creative Commons Attribution (CC BY) license (<http://creativecommons.org/licenses/by/4.0/>).